

Research Article

Severe Inflammation Caused by Coinfection of PCV2 and *Glaesserella parasuis* Is Associated with Pyroptosis via Noncanonical Inflammasome Pathway

Jiahui An , Chao Zhang, Jinshuang Cai, and Yufeng Li 

Key Laboratory of Bacteriology, Ministry of Agriculture, College of Veterinary Medicine, Nanjing Agricultural University, Nanjing 210095, China

Correspondence should be addressed to Yufeng Li; yufengli@njau.edu.cn

Received 6 July 2022; Revised 11 October 2022; Accepted 26 October 2022; Published 16 November 2022

Academic Editor: Shiek Ahmed

Copyright © 2022 Jiahui An et al. This is an open access article distributed under the Creative Commons Attribution License, which permits unrestricted use, distribution, and reproduction in any medium, provided the original work is properly cited.

Coinfections of porcine circovirus type 2 (PCV2) and *Glaesserella parasuis* (*G. parasuis*) are widely existing in the swine industry worldwide. However, the mechanisms for this coinfection remain unclear. The aim of this study is to assess whether the coinfection PCV2 and *G. parasuis* would affect the inflammatory response and related mechanisms. In this study, BALB/c mice and RAW264.7 cells were used to study the inflammation and related mechanism caused by the coinfection of PCV2 and *G. parasuis*. Coinfection with PCV2 and *G. parasuis* significantly increased the mortality of mice and led to the development of more severe lung and spleen lesions compared with single agent infection. Especially, coinfection significantly increased the bacterial loads in the lungs. Coinfection with PCV2 and *G. parasuis* can enhance RAW264.7 cell phagocytosis and elimination to *G. parasuis*. Cell death rate of cells increased in coinfection was measured with Flow cytometry. Moreover, coinfection led to the downregulation of the expression of TNF α and IL-8 in comparison with *G. parasuis* infection, but the maturation of interleukin-1 β (IL-1 β) was significantly upregulated. Our study firstly revealed that coinfection of PCV2 and *G. parasuis* can increase the phagocytosis of cells to *G. parasuis*, and LPS in the cytoplasm will induce the maturation of caspase-11 and lead to the cleavage of Gasdermin D (GSDMD) to cause pyroptosis by noncanonical pathway. The revealing of mechanisms associated with coinfection with PCV2 and *G. parasuis* will provide a scientific basis for investigating the synergistic infection mechanisms between viruses and bacteria.

1. Introduction

Glaesserella parasuis (*G. parasuis*) is a Gram-negative bacterium, which is an important swine pathogen that causes serious diseases, characterized by fibrinous polyserositis, polyarthritis, and meningitis [1]. *G. parasuis* normally colonizes the upper respiratory tract of swine, which can disrupt the nasal mucosal barrier and cause systemic infection in certain conditions [2, 3]. Commonly, *G. parasuis* could coinfect with other pathogens in clinical, such as porcine reproductive and respiratory syndrome virus (PRRSV), porcine circovirus type 2 (PCV2), and *Streptococcus suis* (*S. suis*), and lead to huge economic losses in the swine industry worldwide [4, 5].

PCV2 is a single-stranded, circular, DNA virus; it is the primary pathogen of porcine circovirus-associated disease

(PCVAD) [6, 7]. Additionally, PCV2 is an important immune suppression agent, and it is also a crucial coinfecting agent and increases the risk of infection with other viruses and bacteria [6, 8–10]. Several studies have demonstrated that the infection of PCV2 can aggravate secondary or opportunistic infections in detail [11, 12]. Liu et al. found that *G. parasuis* serovar 4 infection increased the virus loads of PCV2 in the pig sera coinfecting with PCV2 and *G. parasuis* and strengthened lung and lymphoid lesions [13].

Cell death is a fundamental biological phenomenon that is essential for life forms, which was believed to be the result of programmed cell death or uncontrolled cell death [14]. In brief, cells were removed from the tissue in either a programmed manner by a series of molecular and biochemical events or in a poorly uncontrolled manner, resulting in

spillage of cell contents into surrounding tissues and damage thereof [14, 15]. Apoptosis and pyroptosis were both following a programmed series of caspase-dependent events; however, apoptosis was not affecting normal cells and pyroptosis was proinflammation [16, 17]. Apoptosis research is common in PCV2 or *G. parasuis* infection. In previous studies, macrophage apoptosis could be detected in the spleen of PCV2-infected mice, and it also has been reported that apoptosis could be one of the causes of lymphopenia [18, 19]. The lipooligosaccharide of *G. parasuis* played an important role in apoptosis [20]. Nevertheless, there were few studies on PCV2 or *G. parasuis* infection leading to pyroptosis.

Alveolar macrophages (AMs) are the main targets of pulmonary resistance to infection and play key roles in the first line of defense in the immune system [21]. AMs participate in many biological processes, including immune surveillance, tissue repair, and inflammation responses of the lungs [22, 23]. Recent research demonstrated that AM migration is impaired during some viral infections, which will easily lead to secondary bacterial coinfections [24]. Another study showed that swine influenza virus (SIV) can promote the adhesion and invasion in lungs of *S. suis* [25]. Nevertheless, little is learnt about the pulmonary immune responses and associated mechanisms induced by the coinfection of PCV2 and *G. parasuis*.

In this study, BALB/c female mice were used to study the effect of interaction between PCV2 and *G. parasuis* on increasing pathogenicity. RAW264.7 cell line was used to reveal the effect of PCV2 infection on the cell phagocytosis to *G. parasuis in vitro*. At the same time, caspase-11 activation and the noncanonical activation of the inflammasome were confirmed during infections.

2. Materials and Methods

2.1. Virus, Bacteria, and Cell Culture. Virulent PCV2 strain WG09 (GenBank accession no. GQ845027) used in this study was kept in our laboratory, and titers were determined as $10^{6.0}$ TCID₅₀/mL [26]. *G. parasuis* serovar 5 strain used in this study was kept in our laboratory and grown on Tryptone Soy Agar (TSA, OXOID) and Tryptone Soy Broth (TSB, OXOID) with 5% serum and 0.01% NAD. The porcine kidney 15 (PK15) cells and RAW264.7 cells (stored in our lab) used in this study were maintained in Dulbecco Modified Eagle Medium (DMEM) (Gibco, USA) supplemented with 10% fetal bovine serum (FBS, Gibco, USA) and incubated at 37°C with 5% CO₂.

2.2. Animal Infection Experiment. Twenty 8-week-old SPF BALB/c female mice (purchased from the Comparative Medicine Center of Yangzhou University) were randomly divided into four groups and raised in separate facilities, each with 5, the groups including the PCV2 infection group, the *G. parasuis* infection group, the coinfection group, and the PBS control group. The mice were inoculated with 0.2 mL PBS in the control groups and PCV2 ($10^{6.0}$ TCID₅₀/mL) intraperitoneally (IP) in the experimental groups [27]. After 7 days of infection, the mice of the *G. parasuis* single group and the coinfection group were inoculated with *G. parasuis* (4.21×10^9 CFU, per mouse). After infection, clinical symptoms, including depression, huddling,

ruffled fur, and respiratory distress, were recorded until the end of experiment. When the mice were not responsive or recumbent, they were euthanized.

2.3. Histopathological Analysis. When the experimental mice were euthanized, the lung and spleen tissues of each group were freshly collected and fixed in 4% paraformaldehyde and then embedded with paraffin. 5 μm thin tissue sections were prepared, fixed on the glass, and then HE staining was performed for subsequent light microscopy.

2.4. Cell Infection Experiment. RAW264.7 macrophage cells were infected initially with PCV2 for 24 h, and then the cells were infected with *G. parasuis* at an MOI of 100 for 1 h. Then, nonspecifically attached bacteria were removed by washing three times with PBS. Complete growth medium (including 100 U/mL penicillin G and 100 μg/mL gentamycin) was added to each well, and plates were incubated for 1 h to kill extracellular *G. parasuis*. Then, the medium was replaced with fresh complement DMEM containing 10% FBS. The samples for supernatants and lysates were collected at 12 h postinfection. Simultaneously, cells were treated with 10 μM Nigericin (NGC) (MedChemExpress) at 1 h as positive control. Nigericin is an inductor of the canonical way of pyroptosis by caspase-1 [28].

2.5. Cell Death Test. Lactate dehydrogenase (LDH) release was evaluated using an LDH Assay Kit (Beyotime, Shanghai, China) according to the manufacturer's instructions. LDH release reagent treatment (1:10 dilution, 1 hour) was used as a positive control to test maximum LDH release according to the manufacturer's protocol. The optical density was measured spectrophotometrically at 490 nm on a microplate reader.

2.6. Cytokine Expression. The concentration of cytokines in the cell supernatant infected with either PCV2 or *G. parasuis* was determined using ELISA Kit. And the concentration was quantitated based on the standard curves. IL-1β ELISA Kit (absin, abs520001), TNFα ELISA Kit (absin, abs552204), IL-10 ELISA Kit (absin, abs520005), and IL-8 ELISA Kit (Fcmacs Biotech) were used.

Expressions of other cytokines were measured using real-time quantitative PCR (Applied Biosystems, Thermo Fisher Scientific) and calculated using $2^{-\Delta\Delta Ct}$, where CT is the cycle threshold. PCR primers for different cytokines are listed in Table S1.

2.7. Annexin V-FITC/PI Staining for Cell Death. RAW264.7 cells were grown in 12-well plates and treated as previously described. Annexin V-FITC/PI Apoptosis Detection Kit (Vazyme, A211-01) was used for flow cytometry (FC) and fluorescence microscope, and the steps were done according to the instructions. The result analysis was by FlowJo X.

2.8. Western Blot. The cell lysates and supernatants were obtained using RIPA Lysis Buffer containing proteinase inhibitor (Beyotime, Shanghai, China) and acetone precipitation, respectively; the concentration of total proteins was determined using bicinchoninic acid (BCA) protein assay (Beyotime, Shanghai, China). The protein samples were subjected

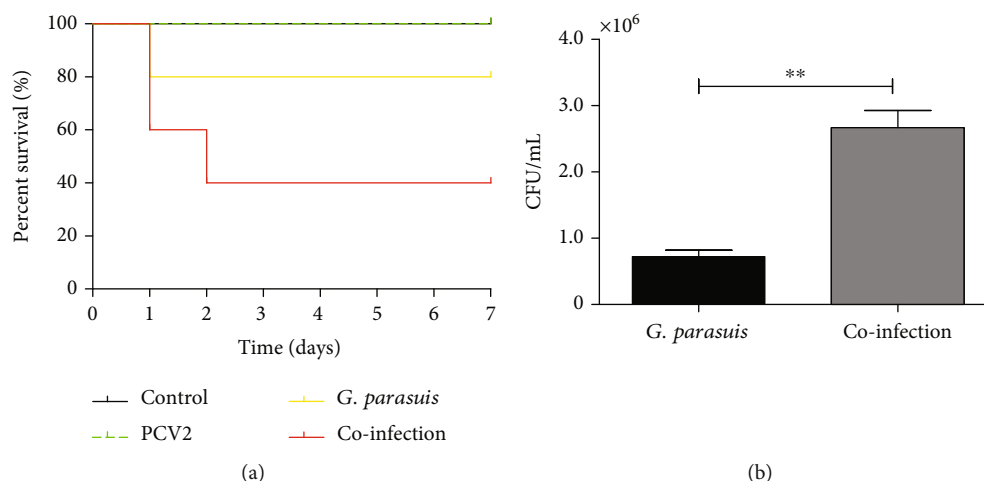


FIGURE 1: Survival rate of experimental mice and bacterial loads in the lungs. (a) The BALB/c mice were inoculated with 0.2 mL PBS or PCV2 ($2 \times 10^{5.0}$ TCID₅₀/mouse) for 7 days, and then, the mice were inoculated with *G. parasuis* (4.21×10^9 CFU/mouse). Mice used as control were treated only with PBS at both time points. (b) Bacterial loads in the lungs. Groups of mice were infected prior with either PCV2 or PBS for 7 days and then challenged with *G. parasuis* (the mice were euthanized at 12 h), and the number of bacteria in the lungs was recorded using CFUs.

to 12.5% SDS-PAGE, and then, they were transferred onto NC membranes (Millipore). After blocking with 5% skim milk for 2 h, the membranes were immunoblotted with primary antibodies overnight at 4°C and then incubated with secondary antibodies for 45 min. Target proteins were exposed with SuperSignal West Pico PLUS (Thermo Fisher Scientific). The band intensity was scanned with ImageJ software, and β -actin was used as housekeeping gene. Primary antibodies include caspase-11 (1:1000, Abcam, ab22684), cleaved caspase-1 (1:1000, Cell signaling technology, 89332), GSDMD (1:800, Abcam, ab219800), and β -actin (1:1000, Santa Cruz Biotechnology, sc47778). Secondary antibodies include goat anti-mouse IgG (H+L) (1:10000, Thermo Fisher Scientific, 31430) and goat anti-rabbit IgG (H+L) (1:1000, Beyotime, A0208).

2.9. Indirect Immunofluorescence Assay. PCV2-infected cells were washed with PBS, fixed with 4% paraformaldehyde for 30 min. Fixed cells were incubated with mouse anti-PCV2-cap protein monoclonal antibody (1:500, preparation in our laboratory) at 37°C for 1 h, washed three times with PBST (0.05% Tween-20 in PBS, pH 7.4), and further incubated with goat anti-mouse IgG (H+L)/FITC (1:50, Bioss, bs0296G-FITC) at 37°C for 1 h in the dark. DAPI was used in the cell nucleus. After three washes with PBST, infected cells were quantified using microscopy.

2.10. Statistical Analysis. All statistical analysis was completed using GraphPad software. Significance was calculated using one-way analysis of variance (ANOVA) with Tukey's post hoc test. *p* value of less than 0.05 was determined to be statistically significant.

3. Results

3.1. Coinfection of PCV2 Virus and *G. parasuis* Bacterium Increases Mouse Mortality. The survival rates of mice for *G. parasuis* infection and coinfection groups are 80% and 40%,

respectively. However, the death of mice was not observed in the control and PCV2 infection groups at the end of the experiments (Figure 1(a)). Additionally, the bacterial loads in the lungs were determined, and as shown in Figure 1(b), the bacterial loads in the lungs from the PCV2 and *G. parasuis* coinfection groups were significantly (***p* = 0.0022) increased compared with *G. parasuis* single infection.

3.2. Coinfection of PCV2 and *G. parasuis* Aggravates Lung and Spleen Injury. Postmortem observations found more tissue lesions in the mice coinfecting with the virus and bacteria, especially for the lungs and spleen. The lungs and spleens were subjected to histopathological examination; the results showed only slight bleeding in the lungs and was observed for PCV2 or *G. parasuis* infection. However, more lung lesions were observed with destroyed alveoli, thickened alveoli septum, and pulmonary congestion in the coinfection group (Figure 2(a)). In addition, the lesions of spleens were not obvious in the postmortem observations, but pathologic observations showed that there were many inflammatory cells infiltrating the spleens in the coinfection group and showed severe lymphocyte depletion and disintegration (Figure 2(b)).

3.3. Effect of Coinfection on Phagocytosis and Clearance by RAW 264.7. In order to confirm whether RAW 264.7 could be infected by PCV2, the cells were infected with PCV2 at a MOI of 1 for 24 h. The mock-infected cells were used as negative control. The cells were then fixed with and incubated with specific antibody against PCV2 and viewed with a fluorescence microscope (Figure S1).

To reveal the effect of coinfection on phagocytosis and clearance by RAW 264.7, a phagocytosis and cell clearance assays for the cells of *G. parasuis* were performed. The results showed that the phagocytosis of RAW 264.7 coinfecting with two agents was significantly increased (3.2 folds, ****p* < 0.0001) than those infected by *G. parasuis* (Figure 3(a)). The number of bacteria in the RAW264.7 cells

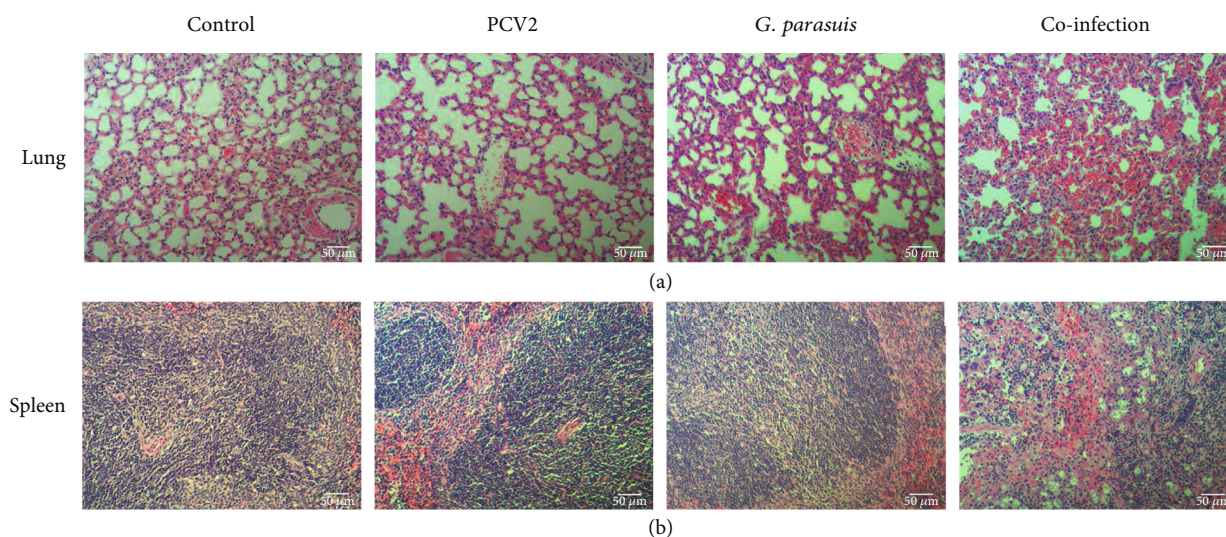


FIGURE 2: Microscopic observations of lungs and spleens. After 12 h of infection with *G. parasuis*, the mice were euthanized. The lungs and spleens were isolated, fixed, stained with HE, and observed by microscopy (scale bar is 50 μm). (a) Lungs showed only slight bleeding and were observed for PCV2 or *G. parasuis* infection, but there were destroyed alveoli, thickened alveoli septum, and pulmonary congestion in the coinfection group. (b) Follicles of the coinfection group were depleted and disintegrated.

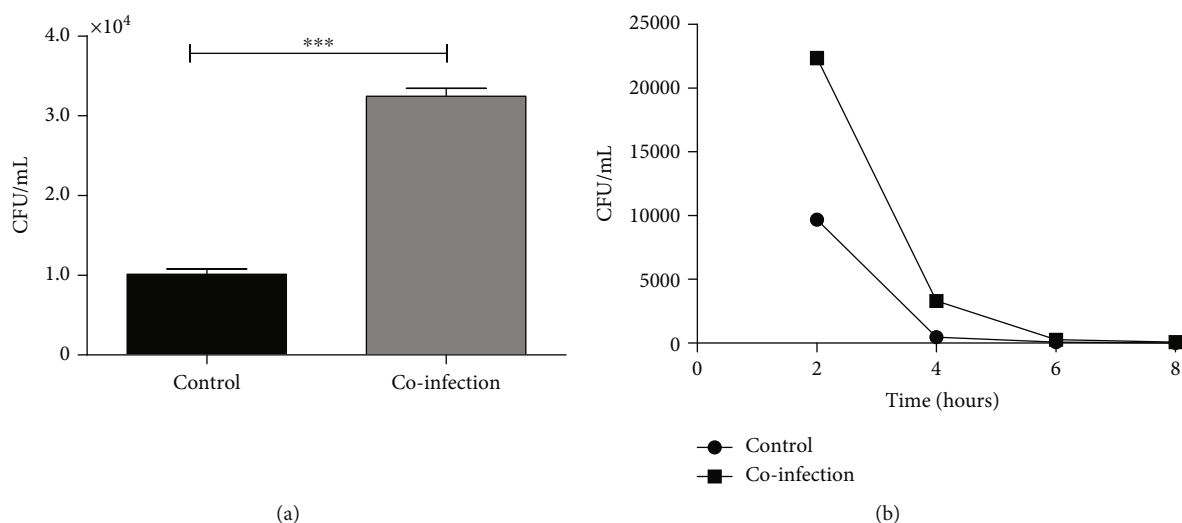


FIGURE 3: Phagocytosis and clearance of *G. parasuis* by RAW 264.7 cells to coinfection with PCV2. (a) RAW264.7 cells were initially infected with PCV2 (MOI = 1) for 24 h and then infected with *G. parasuis* (MOI = 100) for 1 h, and the medium was replaced with fresh complement DMEM containing penicillin and gentamicin for 1 h, and then, the cells were washed, lysed, and streaked onto TSA for CFU count. (b) The treated RAW264.7 cells were lysed and streaked onto TSA for CFU count at 2 h, 4 h, 6 h, and 8 h, respectively.

was recorded at different time points following infection, and this result showed that the elimination rate of bacteria was increased in the coinfection group (Figure 3(b)).

3.4. Regulation of Cytokine Expression in the RAW 264.7 Cells Coinfected with PCV2 and *G. parasuis*. The expressions of some selected inflammation-relevant genes were analysed after different infections. The groups for PCV2 and *G. parasuis* coinfection and single *G. parasuis* infection induced the expression of TNF- α , IL-8, IL-10, and IL-1 β increased at protein levels (Figure 4). However, a significant downregulation of TNF- α and IL-8 levels was detected after coinfection at 12 h compared with the group infected only with *G. parasuis*

and PCV2 (Figure 4(a)). IL-10 expression had no significant differences being found between the *G. parasuis* infection and coinfection at 6 h or 12 h. IL-1 β expression was higher in the coinfection group at 12 h. Results of measurement of mRNA levels are in the supplementary material (Figure S2).

3.5. Pyroptosis of RAW264.7 Associated with Coinfection of PCV2 and *G. parasuis*. Cell viability results showed that coinfection caused more cell damage by increasing the release of LDH (Figure 5(a)), which may be associated with inflammatory responses of cells. To explore the relationship between cell viability and inflammatory response of RAW264.7 cells, the secretion of mature IL-1 β into the cell supernatant was

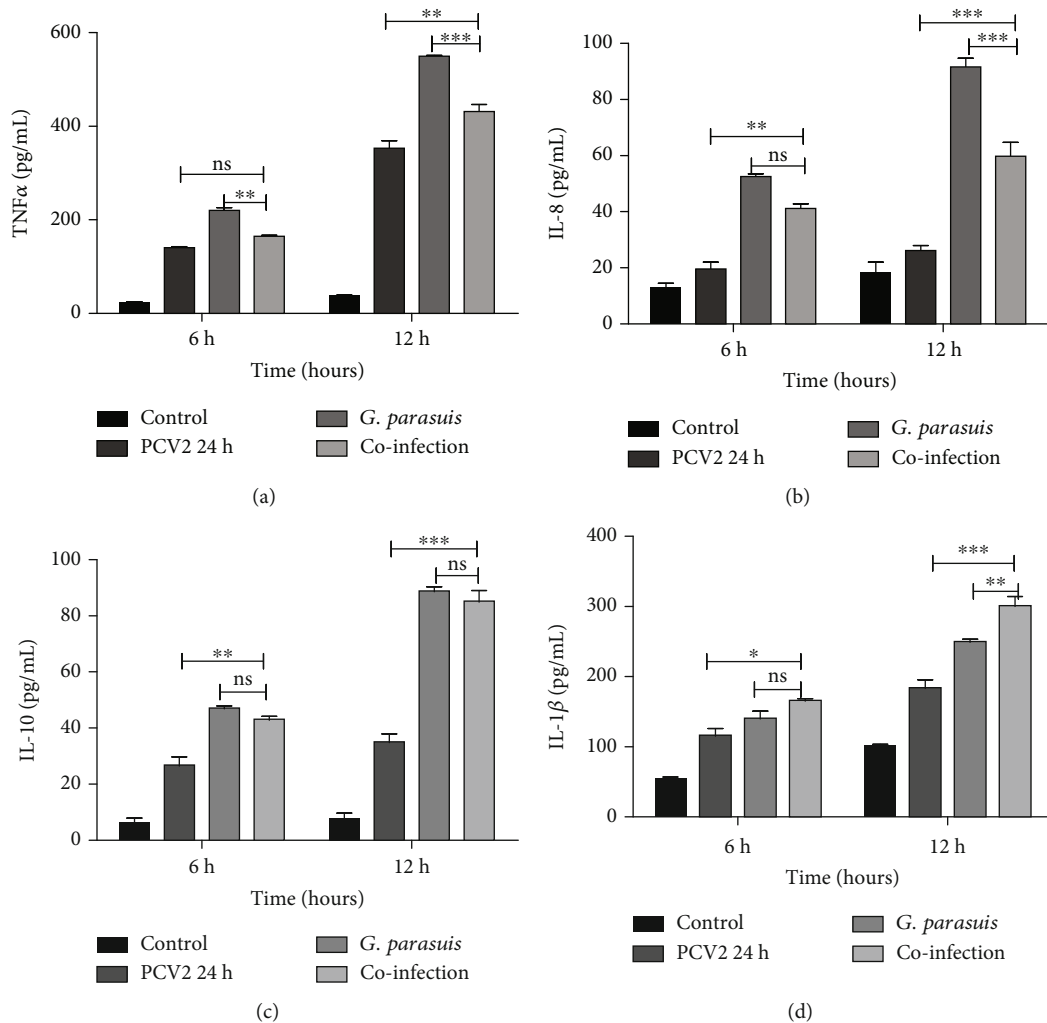


FIGURE 4: The protein levels of some inflammation-related cytokines in RAW264.7 after infection. RAW264.7 cells were infected prior with PCV2 (MOI = 1) for 24 h and then infected with *G. parasuis* at an MOI of 100 for 1 h. After treatment with penicillin and gentamicin for 1 h, the cells were replenished with complete medium and were further cultured; then cell culture supernatant was collected at 6 h and 12 h. (a) TNF α expression level, (b) IL-8 expression level, (c) IL-10 expression level, and (d) IL-1 β expression level (** $p < 0.01$, *** $p < 0.001$, and * $p < 0.05$).

monitored. We found that *G. parasuis* infection and coinfection can activate mature IL-1 β secretion (Figure 5(b)), which is positively associated with LDH release at 12 h.

3.6. Coinfection of PCV2 and *G. parasuis*-Induced Cell Death. Annexin V-FITC/PI was used for estimating better the relative contribution of the different cell death mechanisms. For flow cytometry analysis, four rectangle gates depended on the control and positives groups. The results showed that 6.94% cells after NGC treatment (Figure 6(d)), 5.35% cells after PCV2 infection (Figure 6(a)), 5.92% cells after *G. parasuis* infection (Figure 6(b)), and 4.95% cells after coinfections (Figure 6(c)) were in early apoptosis (FITC-positive), and the proportion of late apoptotic and necrotic cells (FITC and PI double positive) was 12.6% (Figure 6(d)), 12.7% (Figure 6(a)), 11.4% (Figure 6(b)), and 11.8% (Figure 6(c)) in each of these groups. In addition, the single positive rate of the cell nucleus (PI positive) in the PCV2, *G. parasuis*, coinfection, and NGC groups was 3.90% (Figure 6(a)), 5.37% (Figure 6(b)), 6.82% (Figure 6(c)), and 23.7%

(Figure 6(d)), respectively. These results were similar to fluorescence determined (Figure S3).

3.7. Caspase-11 Activation and GSDMD Lysis. More bacteria were phagocytized in the group coinfecting with PCV2 and *G. parasuis* than that in the group infected with *G. parasuis* only, which would lead to more cytosolic LPS in the coinfecting cells. As is well known, cytosolic LPS was sensed by caspase-11 during Gram-negative bacterial infections [29]. To test whether caspase-11 is activated by *G. parasuis*, caspase-11 expression and cleavage were identified by western blotting. We found that the cleavage of caspase-11 was significantly increased by coinfection (Figure 7). NGC did not affect the expression and activation of caspase-11.

To determine whether coinfection could affect the activation of the noncanonical inflammasome signaling pathway, the expression of cleavage GSDMD was detected by western blot. As shown in Figure 8, coinfection could significantly upregulate cleavage GSDMD in RAW264.7 cells. NGC also induced the expression of cleavage GSDMD. This result

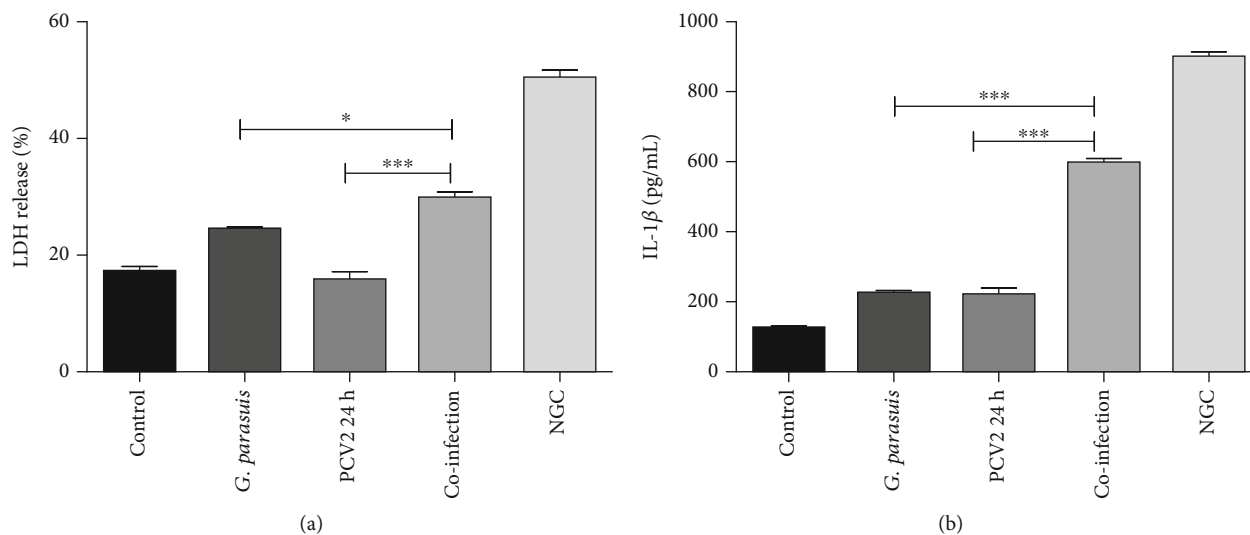


FIGURE 5: IL-1 β and LDH release. LDH release (a) and IL-1 β expression (b) by RAW264.7 cells coinfecting with PCV2 and *G. parasuis* in comparison with those infected with PCV2 (MOI = 1) and *G. parasuis* (MOI = 100) and stimulated with 10 μ M Nigericin (NGC) for 1 h (*** p < 0.001, ** p < 0.01, and * p < 0.05).

indicated that coinfection could enhance pyroptosis by the noncanonical inflammasome signaling pathway.

4. Discussion

Coinfection of PCV2 and *G. parasuis* is a common clinical incident associated with significant economic losses to the swine industry [10, 30, 31]. However, PCV2 infection is easy to be ignored or underestimated for mainly causing asymptomatic or mild clinical signs by itself [6]. *G. parasuis* is an opportunistic pathogen that colonizes the upper respiratory tract and typically complicates infections by other primary pathogens, worsening the production performance [1, 32]. To date, the synergistic infection mechanisms between PCV2 and *G. parasuis* have not been well studied. BALB/c mice and RAW264.7 cells are the common and convenient models for studying PCV2 infection [27, 33]. Despite BALB/c mice being regarded as an inadequate model for virulence of serovar 5 strain of *G. parasuis* [34], the fact does not affect the relevance of the reported data because the mechanism was studied, which may be independent from the virulence of *G. parasuis*. In this study, the results of BALB/c mice infected with PCV2 and *G. parasuis* demonstrated that PCV2 and *G. parasuis* have synergistic interactions in pathology and PCV2 infection can increase *G. parasuis* propagation in the lungs. Moreover, coinfection enhances the activation of caspase-11 and cleavage of GSDMD, which is associated with pyroptosis via the noncanonical inflammasome signaling pathway *in vitro*.

The most significant microscopic lesions in PCV2-associated infected pigs are in lymphoid organs, and the spleen is the largest secondary lymphoid organ in the body, which contains large number of lymphocytes [3, 18, 35]. Therefore, the spleen was observed, and the follicles of the spleen showed severe lymphocyte depletion and disintegration in the coinfection group but not in other groups. This is probably due to the enhanced pathogenicity of coinfection. The previous study showed that coinfection of PCV2 and HPS4 (*G. parasuis*) could

decrease the number of lymphocytes [13], and the lesions of the spleen might also be the cause of the reduction of lymphocytes. Monocyte/macrophage lineage cells are major target cells of PCV2 [36]. Bacterial lipopolysaccharide (LPS) induced PCV2 replication in swine alveolar macrophages [37]. Hence, we also examined the effects of infection in lungs by microsection and found that coinfection could lead more serious lung injury.

Lung inflammation caused by pathogenic infections is often accompanied by overexpression of various cytokines, which leads to severe lung damage and high mortality [38, 39]. Cytokines play a very complex role in pathogen infection [40]. As shown in our study, the cytokine IL-1 β was highly expressed in coinfection at 12 h. However, RAW 264.7 cells coinfecting with PCV2 and *G. parasuis* decreased the expression of TNF α and IL-8 cytokines compared with cells infected with *G. parasuis* at 12 h. Downregulation of proinflammatory cytokine expression in RAW264.7 cells is similar to that of alveolar macrophages (PAMs) coinfecting with porcine reproductive and respiratory syndrome virus (PRRSV) and *G. parasuis* [41]. These results may suggest that the immunological responses to bacterial infection in the coinfecting group are downregulated, which affects the recruitment of other immune cells [42].

Pyroptosis is a highly specific type of inflammatory programmed cell death that is different from necrosis or apoptosis [43, 44], and it is regulated by caspase-1 dependent or independent mechanisms [44]. Caspase-1 is activated upon various infections, belonging to the inflammatory caspase group, which distinguishes pyroptosis from apoptosis [45]. In caspase-1-independent mechanism, cytosolic LPS (from Gram-negative bacteria) is recognized by caspase-11 rather than caspase-1 in mouse cells. Besides that, these inflammatory caspases directly cleaved GSDMD and induced pyroptosis. The N-terminal fragment also activates the NLRP3 inflammasome and caspase-1-dependent maturation of IL-1 β . *G. parasuis* has been shown to activate caspase-1 and NLRP3 through toll-like receptor [38]. In this study, we removed the *G. parasuis* after 1 h infection and collected the samples at 12 h; the activation of

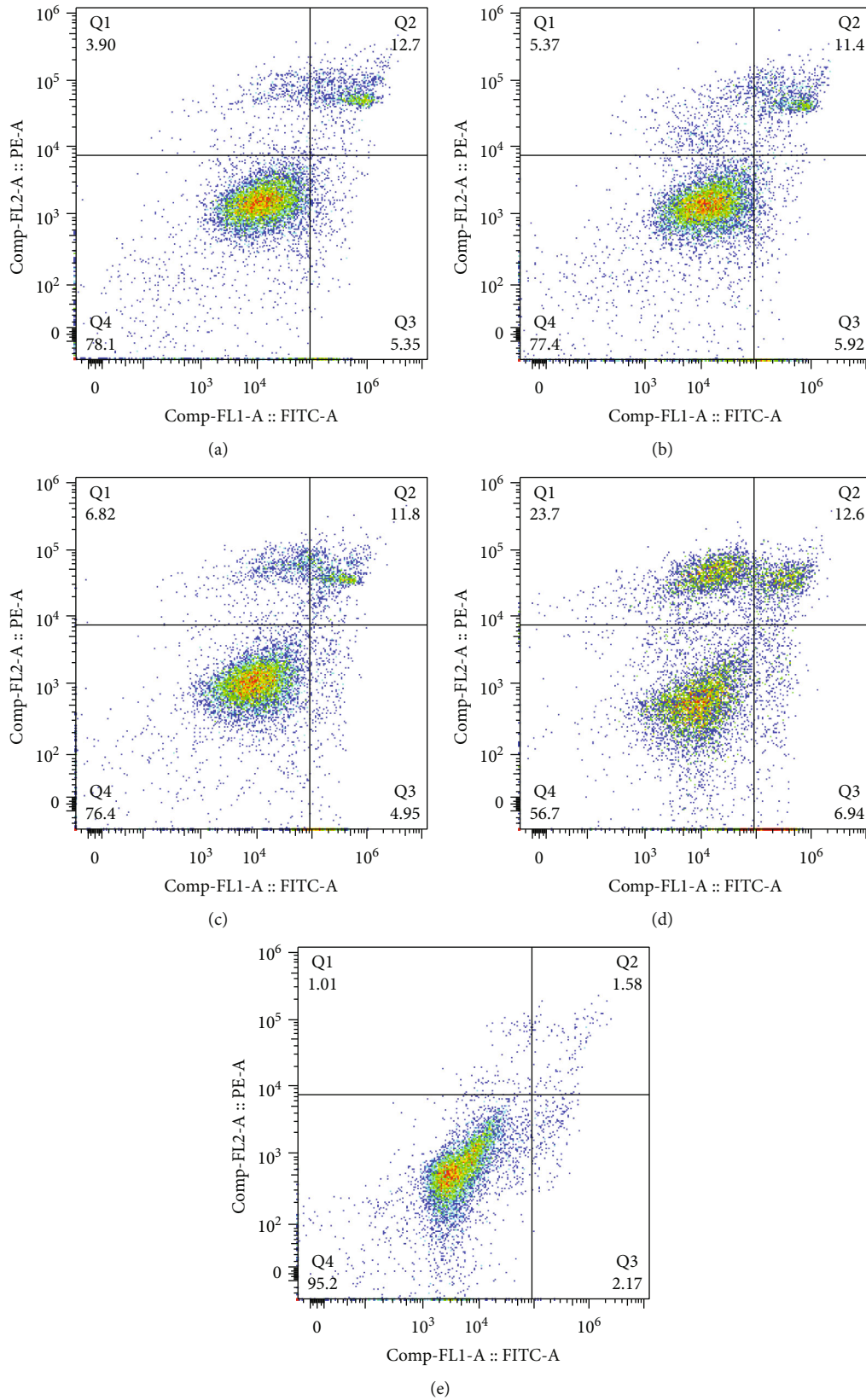


FIGURE 6: Coinfection of PCV2 and *G. parasuis*-induced cell death. (a) PCV2 24h infection group. (b) *G. parasuis* 12h infection group. (c) Coinfection group. (d) Nigericin (NGC) 1h treated group. (e) Negative control. Stimulated with 10 μ M Nigericin (NGC) for 1h as positive control. Gate Q1 means PI single positive, Q2 means FITC and PI double positive, Q3 means FITC single positive, and Q4 means FITC and PI double negative.

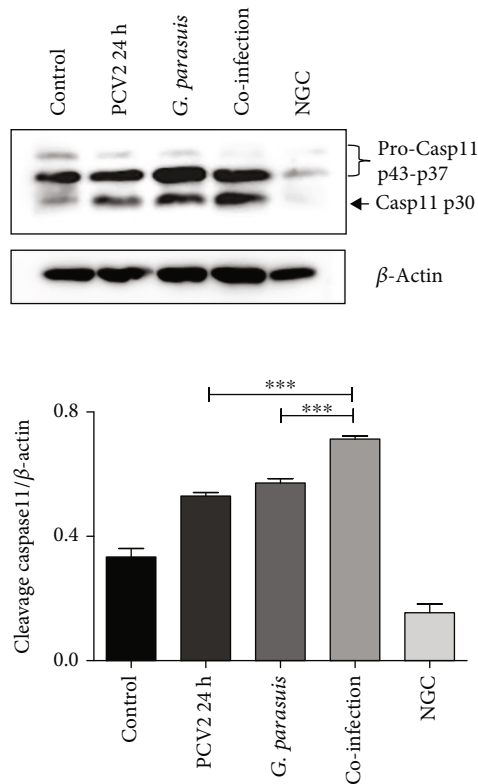


FIGURE 7: Intracellular *G. parasuis* sensing leads to the activation of caspase-11 in RAW264.7 cells. The activation of caspase-11 was identified using western blotting with the indicated antibodies. Data are representatives of three independent experiments with similar results. Stimulated with 10 μ M Nigericin (NGC) for 1 h as control (** $p < 0.01$, and * $p < 0.05$).

caspase-1 was not significant between the *G. parasuis* group and the coinfection group (Figure S4); however, there is difference between the *G. parasuis* and coinfection groups in expression of cleavage GSDMD, so other reasons should be further considered. In this study, the number of *G. parasuis* phagocytized by the cells increased significantly after the PCV2 preinfection. This suggested that LPS in the cytoplasm was also increased. The noncanonical inflammasome, triggered pyroptosis by activating caspase-11, is related to LPS in the cytoplasm [46]. This reminds us coinfection may cause cell death by caspase-1-independent way. Therefore, we tested the cleavage fragment expression of GSDMD, and the result showed that the cleavage of GSDMD in the coinfection group significantly increased. So, we can make a conclusion that coinfection can cause pyroptosis of cells, which may be associated with more severe systemic inflammation of pigs coinfecting with PCV2 and *G. parasuis* compared with single infection.

We mainly focused on the effect of secondary *G. parasuis* infection with PCV2 preceding infection. The success of this study laid an important theoretical basis and provides necessary experimental means for discussing the secondary infection of other pathogens caused by PCV2 infection and also provided an important theoretical basis for the scientific and effective prevention and control of PCVAD and Glässer's disease.

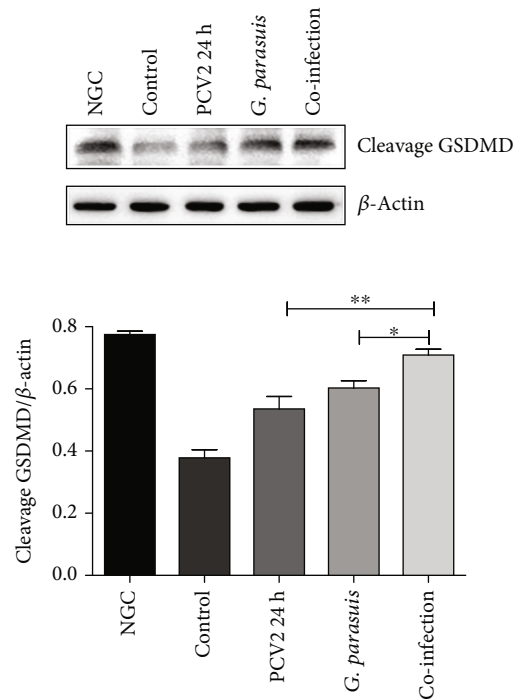


FIGURE 8: The cleavage of GSDMD in infection. The cleavage of GSDMD was identified by western blotting with the anti-cleaved GSDMD antibody and β -actin antibody. Data are representatives of three independent experiments with similar results. Stimulated with 10 μ M Nigericin (NGC) for 1 h as control (** $p < 0.001$, ** $p < 0.01$, and * $p < 0.05$).

5. Conclusion

We can conclude that coinfection of PCV2 and *G. parasuis* can increase the phagocytosis of cells to *G. parasuis* and cell death. LPS (from *G. parasuis*) in the cytoplasm will induce the maturation of caspase-11 and lead to the cleavage of GSDMD to cause pyroptosis. As it is well known that pyroptosis is positively associated with inflammation responses. Our study revealed for the first time that a more severe disease is caused by the combination of PCV2 and *G. parasuis* infections, which increases inflammation by upregulation of non-canonical pathway.

Data Availability

The data that support the findings of this study are available from the corresponding author upon reasonable request. And the data presented in the manuscript is available as part of this manuscript and as supplementary information.

Ethical Approval

All animal experiments were performed in the Laboratory Animal Center of Nanjing Agricultural University with the approval of the Department of Science and Technology of Jiangsu Province (Permit number: SCXK (SU) 2017-0007). All experimental procedures were conformed to institutional guidelines in accordance with international law, and all efforts were made to minimize suffering.

Conflicts of Interest

There are no competing interests to declare.

Authors' Contributions

Jiahui An was responsible for the conceptualization, methodology, writing, and original draft; Chao Zhang was responsible for the visualization and formal analysis; Jinshuang Cai was responsible for the validation and formal analysis; Yufeng Li was responsible for the resources, funding acquisition, and project administration.

Acknowledgments

This study was supported by the National Key Research and Development Program of China (2017YFD0500102), the National Natural Science Foundation (31672565), and the Priority Academic Program Development of Jiangsu Higher Education Institutions (PAPD).

Supplementary Materials

Supplementary 1. Figure S1: the infection of PCV2 to RAW 264.7.

Supplementary 2. Figure S2: the mRNA levels of some inflammation-related cytokines in RAW264.7 after infection.

Supplementary 3. Figure S3: Annexin V-FITC/PI staining for cell death.

Supplementary 4. Figure S4: the activation of caspase-1.

Supplementary 5. Table S1: primers used for real-time PCR quantification of gene expression.

References

- [1] S. Oliveira and C. Pijoan, "Haemophilus parasuis: new trends on diagnosis, epidemiology and control," *Veterinary Microbiology*, vol. 99, no. 1, pp. 1–12, 2004.
- [2] C. A. Lichtensteiger and E. R. Vimr, "Purification and renaturation of membrane neuraminidase from *Haemophilus parasuis*," *Veterinary Microbiology*, vol. 93, no. 1, pp. 79–87, 2003.
- [3] B. E. Straw, Z. Jeffrey, D. Sylvie, and D. J. Taylor, *Diseases of swine*, John Wiley & Sons, 9th Ed edition, 2013.
- [4] C. Salogni, M. Lazzaro, S. Giovannini et al., "Causes of swine polyserositis in a high-density breeding area in Italy," *Journal of Veterinary Diagnostic Investigation*, vol. 32, no. 4, pp. 594–597, 2020.
- [5] G. I. Solano, J. Segalés, J. E. Collins, T. W. Molitor, and C. Pijoan, "Porcine reproductive and respiratory syndrome virus (PRRSv) interaction with *Haemophilus parasuis*," *Veterinary Microbiology*, vol. 55, no. 1-4, pp. 247–257, 1997.
- [6] J. Gillespie, T. Opriessnig, X. J. Meng, K. Pelzer, and V. Buechner-Maxwell, "Porcine circovirus type 2 and porcine circovirus-associated disease," *Journal of Veterinary Internal Medicine*, vol. 23, no. 6, pp. 1151–1163, 2009.
- [7] X. J. Meng, "Porcine circovirus type 2 (PCV2): pathogenesis and interaction with the immune system," *Annual Review of Animal Biosciences*, vol. 1, no. 1, pp. 43–64, 2013.
- [8] C. Chae, "Porcine respiratory disease complex: interaction of vaccination and porcine circovirus type 2, porcine reproductive and respiratory syndrome virus, and *Mycoplasma hyopneumoniae*," *Veterinary Journal*, vol. 212, pp. 1–6, 2016.
- [9] D. Kim, Y. Ha, Y. Oh, and C. Chae, "Prevalence of porcine circovirus types 2a and b in pigs with and without post-weaning multi-systemic wasting syndrome," *Veterinary Journal*, vol. 188, no. 1, pp. 115–117, 2011.
- [10] F. J. Pallares, P. G. Halbur, T. Opriessnig et al., "Porcine circovirus type 2 (PCV-2) coinfections in US field cases of post-weaning multisystemic wasting syndrome (PMWS)," *Journal of Veterinary Diagnostic Investigation*, vol. 14, no. 6, pp. 515–519, 2002.
- [11] C. Fablet, C. Marois, V. Dorenlor et al., "Bacterial pathogens associated with lung lesions in slaughter pigs from 125 herds," *Research in Veterinary Science*, vol. 93, no. 2, pp. 627–630, 2012.
- [12] H. Zhu, X. Chang, J. Zhou et al., "Co-infection analysis of bacterial and viral respiratory pathogens from clinically healthy swine in eastern China," *Veterinary Medicine and Science*, vol. 7, no. 5, pp. 1815–1819, 2021.
- [13] S. Liu, W. Li, Y. Wang et al., "Coinfection with *Haemophilus parasuis* serovar 4 increases the virulence of porcine circovirus type 2 in piglets," *Virology Journal*, vol. 14, no. 1, p. 227, 2017.
- [14] M. S. D'Arcy, "Cell death: a review of the major forms of apoptosis, necrosis and autophagy," *Cell Biology International*, vol. 43, no. 6, pp. 582–592, 2019.
- [15] J. F. Kerr, A. H. Wyllie, and A. R. Currie, "Apoptosis: a basic biological phenomenon with wide-ranging implications in tissue kinetics," *British Journal of Cancer*, vol. 26, no. 4, pp. 239–257, 1972.
- [16] L. H. Boise and C. M. Collins, "Salmonella-induced cell death: apoptosis, necrosis or programmed cell death?," *Trends in Microbiology*, vol. 9, no. 2, pp. 64–67, 2001.
- [17] S. L. Fink and B. T. Cookson, "Apoptosis, pyroptosis, and necrosis: mechanistic description of dead and dying eukaryotic cells," *Infection and Immunity*, vol. 73, no. 4, pp. 1907–1916, 2005.
- [18] M. Kiupel, G. W. Stevenson, E. J. Galbreath, A. North, H. HogenEsch, and S. K. Mittal, "Porcine circovirus type 2 (PCV2) causes apoptosis in experimentally inoculated BALB/c mice," *BMC Veterinary Research*, vol. 1, no. 1, p. 7, 2005.
- [19] A. R. Resendes, N. Majó, J. Segalés, E. Mateu, M. Calsamiglia, and M. Domingo, "Apoptosis in lymphoid organs of pigs naturally infected by porcine circovirus type 2," *The Journal of General Virology*, vol. 85, no. 10, pp. 2837–2844, 2004.
- [20] B. Bouchet, G. Vanier, M. Jacques, E. Auger, and M. Gottschalk, "Studies on the interactions of *Haemophilus parasuis* with porcine epithelial tracheal cells: Limited role of LOS in apoptosis and pro-inflammatory cytokine release," *Microbial Pathogenesis*, vol. 46, no. 2, pp. 108–113, 2009.
- [21] A. Olvera, M. Ballester, M. Nofrarias, M. Sibila, and V. Aragon, "Differences in phagocytosis susceptibility in *Haemophilus parasuis* strains," *Veterinary Research*, vol. 40, no. 3, p. 24, 2009.
- [22] A. J. Byrne, S. A. Mathie, L. G. Gregory, and C. M. Lloyd, "Pulmonary macrophages: key players in the innate defence of the airways," *Thorax*, vol. 70, no. 12, pp. 1189–1196, 2015.
- [23] P. J. Murray and T. A. Wynn, "Protective and pathogenic functions of macrophage subsets," *Nature Reviews Immunology*, vol. 11, no. 11, pp. 723–737, 2011.

- [24] A. S. Neupane, M. Willson, A. K. Chojnacki et al., "Patrolling alveolar macrophages conceal bacteria from the immune system to maintain homeostasis," *Cell*, vol. 183, no. 1, pp. 110–125.e11, 2020.
- [25] F. Meng, N. H. Wu, A. Nerlich, G. Herrler, P. Valentin-Weigand, and M. Seitz, "Dynamic virus-bacterium interactions in a porcine precision-cut lung slice coinfection model: swine influenza virus paves the way for *Streptococcus suis* infection in a two-step process," *Infection and Immunity*, vol. 83, no. 7, pp. 2806–2815, 2015.
- [26] J. Liu, J. Bai, L. Zhang, C. Hou, Y. Li, and P. Jiang, "Proteomic alteration of PK-15 cells after infection by porcine circovirus type 2," *Virus Genes*, vol. 49, no. 3, pp. 400–416, 2014.
- [27] T. Ouyang, X. H. Liu, H. S. Ouyang, and L. Z. Ren, "Mouse models of porcine circovirus 2 infection," *Animal Models and Experimental Medicine*, vol. 1, no. 1, pp. 23–28, 2018.
- [28] S. Mariathasan, D. S. Weiss, K. Newton et al., "Cryopyrin activates the inflammasome in response to toxins and ATP," *Nature*, vol. 440, no. 7081, pp. 228–232, 2006.
- [29] N. Kayagaki, S. Warming, M. Lamkanfi et al., "Non-canonical inflammasome activation targets caspase-11," *Nature*, vol. 479, no. 7371, pp. 117–121, 2011.
- [30] X. Cai, H. Chen, P. J. Blackall et al., "Serological characterization of *Haemophilus parasuis* isolates from China," *Veterinary Microbiology*, vol. 111, no. 3-4, pp. 231–236, 2005.
- [31] J. Kim, H. K. Chung, T. Jung, W. S. Cho, C. Choi, and C. Chae, "Postweaning multisystemic wasting syndrome of pigs in Korea: prevalence, microscopic lesions and coexisting microorganisms," *The Journal of Veterinary Medical Science*, vol. 64, no. 1, pp. 57–62, 2002.
- [32] M. Costa-Hurtado, E. Barba-Vidal, J. Maldonado, and V. Aragon, "Update on Glasser's disease: how to control the disease under restrictive use of antimicrobials," *Veterinary Microbiology*, vol. 242, article 108595, 2020.
- [33] H. L. Chen, H. L. Tan, J. Yang, Y. Y. Wei, and T. J. Hu, "Sargassum polysaccharide inhibits inflammatory response in PCV2 infected- RAW264.7 cells by regulating histone acetylation," *Carbohydrate Polymers*, vol. 200, pp. 633–640, 2018.
- [34] B. Qi, F. Li, K. Chen et al., "Comparison of the *Glaesserella parasuis* virulence in mice and piglets," *Frontiers in Veterinary Science*, vol. 8, 2021.
- [35] S. M. Lewis, A. Williams, and S. C. Eisenbarth, "Structure and function of the immune system in the spleen," *Science Immunology*, vol. 4, no. 33, 2019.
- [36] C. Rosell, J. Segalés, J. Plana-Duran et al., "Pathological, immunohistochemical, and in-situ hybridization studies of natural cases of postweaning multisystemic wasting syndrome (PMWS) in pigs," *Journal of Comparative Pathology*, vol. 120, no. 1, pp. 59–78, 1999.
- [37] H. W. Chang, V. F. Pang, L. J. Chen, M. Y. Chia, Y. C. Tsai, and C. R. Jeng, "Bacterial lipopolysaccharide induces porcine circovirus type 2 replication in swine alveolar macrophages," *Veterinary Microbiology*, vol. 115, no. 4, pp. 311–319, 2006.
- [38] X. Luo, X. Chang, H. Zhou, H. Lin, and H. Fan, "*Glaesserella parasuis* induces inflammatory response in 3D4/21 cells through activation of NLRP3 inflammasome signaling pathway via ROS," *Veterinary Microbiology*, vol. 256, article 109057, 2021.
- [39] S. Wang, N. Jiang, W. Shi et al., "Co-infection of H9N2 influenza A virus and *Escherichia coli* in a BALB/c mouse model aggravates lung injury by synergistic effects," *Frontiers in Microbiology*, vol. 12, article 670688, 2021.
- [40] L. C. Borish and J. W. Steinke, "2. Cytokines and chemokines," *Journal of Allergy and Clinical Immunology*, vol. 111, no. 2, pp. S460–S475, 2003.
- [41] L. Kavanová, K. Matiašková, L. Levá et al., "Concurrent infection of monocyte-derived macrophages with porcine reproductive and respiratory syndrome virus and *Haemophilus parasuis*: a role of IFN α in pathogenesis of co-infections," *Veterinary Microbiology*, vol. 225, pp. 64–71, 2018.
- [42] W. Qi, R. Zhu, C. Bao et al., "Porcine circovirus type 2 promotes *Actinobacillus pleuropneumoniae* survival during coinfection of porcine alveolar macrophages by inhibiting ROS production," *Veterinary Microbiology*, vol. 233, pp. 93–101, 2019.
- [43] X. Ge, W. Li, S. Huang et al., "The pathological role of NLRs and AIM2 inflammasome-mediated pyroptosis in damaged blood-brain barrier after traumatic brain injury," *Brain Research*, vol. 1697, pp. 10–20, 2018.
- [44] S. M. Man, R. Karki, and T. D. Kanneganti, "Molecular mechanisms and functions of pyroptosis, inflammatory caspases and inflammasomes in infectious diseases," *Immunological Reviews*, vol. 277, no. 1, pp. 61–75, 2017.
- [45] J. Shi, W. Gao, and F. Shao, "Pyroptosis: Gasdermin-mediated programmed necrotic cell death," *Trends in Biochemical Sciences*, vol. 42, no. 4, pp. 245–254, 2017.
- [46] J. Ding and F. Shao, "SnapShot: the noncanonical Inflammasome," *Cell*, vol. 168, no. 3, pp. 544–544.e1, 2017.